

# Chapter 3

## Polarization Properties of Prisms and Reflectors

### 3.1 Prisms Producing Polarized Light

#### 3.1.1 Uniaxial double-refracting crystals

Certain types of crystals, such as calcite (Iceland spar or calcium carbonate) exhibit the property of double refraction or *birefringence*, as first observed in calcite by Erasmus Bartholinus in 1669. For the class of crystals called *uniaxial*, there is only one direction where all light rays travel along the same path at a constant velocity. This direction defines the optic axis or principal axis, and any plane that contains the optic axis is called a *principal plane* (sometimes called a *principal section*). The optic axis is not a specific line, but indicates a direction in the crystal where there is no double refraction. For all rays not traveling along the optic axis, the velocity is determined by a pair of refractive indices called the ordinary refractive index  $n_o$  and the extraordinary refractive index  $n_e$ , and the path of an incident ray is split into two rays, the so-called o-rays and e-rays. Birefringence is specified by the number  $(n_o - n_e)$ . Moreover, these o-rays and e-rays are polarized and vibrate in mutually perpendicular planes. Only rays traveling parallel to the optic axis will not be split, and  $n_o$  is therefore assigned to this direction. One way to represent this refractive index variation is by use of the *indicatrix*.<sup>1</sup> Figure 3.1(a) shows a positive uniaxial indicatrix in the shape of an oblate spheroid, where  $n_e > n_o$ , and Fig. 3.1(b) shows a negative uniaxial indicatrix in the shape of a prolate spheroid, where  $n_o > n_e$ . Both have circular symmetry in planes normal to the optic axis, and when the indicatrix has a spherical shape,  $n_e = n_o$ , and the crystal is isotropic.

#### 3.1.2 Nicol polarizing prism

One of the first prism polarizers to utilize a birefringent crystal was developed by William Nicol in 1828 and is known as the Nicol prism. The Nicol prism shown in Fig. 3.2 is constructed from negative uniaxial calcite, where  $n_o = 1.6584$  and  $n_e = 1.4864$  for  $\lambda = 589.3$  nm. Calcite is a widely used material because of its clarity, stability, high spectral transmission range (200–5000 nm), and high birefringence. Two triangular sections are optically coupled at the hypotenuse by a thin coating of optically clear cement such as Canadian balsam ( $n_{\text{cement}} \approx 1.54$ ),

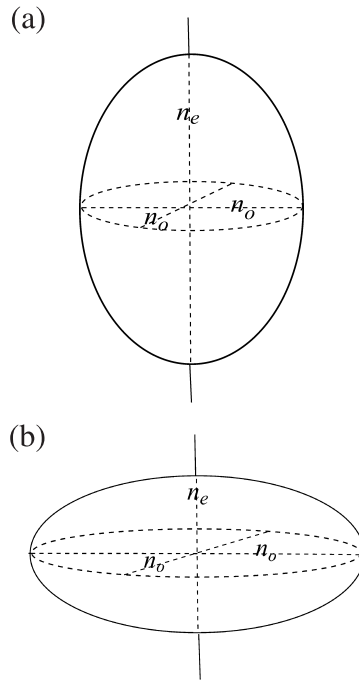


**Figure 3.1** (a) Positive uniaxial indicatrix ( $n_e > n_o$ ). (b) Negative uniaxial indicatrix ( $n_o > n_e$ ).

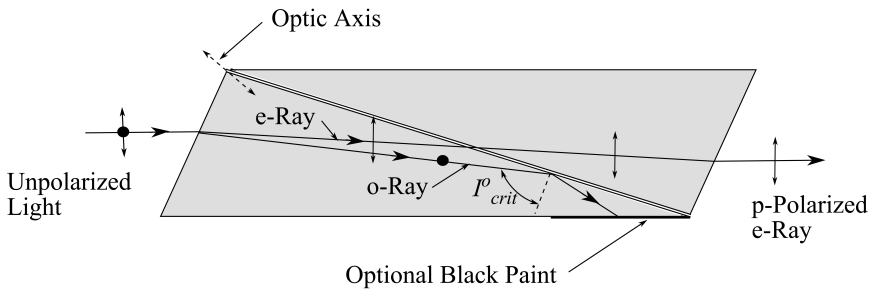


**Figure 3.2** Nicol prism polarizer made of calcite,  $n_o = 1.6584$ ,  $n_e = 1.4864$ .

with the optic axis direction as shown. An incident unpolarized ray is split at the entrance surface, with both rays becoming linearly polarized. By controlling the incident angle of the rays at the interface, the o-ray can undergo total internal reflection (TIR), where  $I^o_{crit} = \arcsin(n_{cement}/n_o) \approx 68$  deg. Since  $n_{cement} > n_e$ , the e-ray is always transmitted and exits the prism as linearly polarized light. This separation of o-rays and e-rays by TIR is a useful technique that is used in other types of polarizing prisms. Although the exit ray is parallel to the incident ray, there is a slight lateral displacement (noncollinear), the angular field is limited, and the interface cement will suffer damage at high power levels.

### 3.1.3 Glan–Foucault polarizing prism

One of several Glan-type polarizing prisms is the Glan–Foucault prism, shown in Fig. 3.3(a). The calcite prisms are air spaced at the interface, and each optic axis is perpendicular to the plane of reflection. There is no separation of the ray paths in the first prism section, but the o-ray moves slower in the first section and undergoes retardance with respect to the e-ray. Again, TIR is used to separate the o-ray from the e-ray, and s-polarized light is emitted from the exit face. The o-ray is usually absorbed by blackening the side face. The field of view is determined by TIR failure of the o-ray at the glass–air interface 2, or TIR of the e-ray at this interface. For calcite,  $n_o = 1.6557$  and  $n_e = 1.4852$  at  $\lambda = 630$  nm. The corresponding critical angles are  $I_{crit}^o = 37.16$  deg and  $I_{crit}^e = 42.32$  deg. As shown in Fig. 3.3(b), the maximum angle of incidence  $I_1^o$  for the o-ray at entrance surface 1 is estimated by  $I_{1max}^o = \arcsin[n_o \sin(38.5 \text{ deg} - I_{crit}^o)] \approx 2.4$  deg. The maximum angle of incidence  $I_1^e$  for the e-ray is estimated by  $I_{1max}^e = \arcsin[n_o \sin(I_{crit}^e - 38.5 \text{ deg})] \approx 6.3$  deg. This results in a narrow asymmetric field of view about the central axis in the tangential plane. A nominal angular field is given as 6 deg at  $\lambda = 633$  nm by a commercial supplier of the Glan–Foucault prism, United Crystals Company.

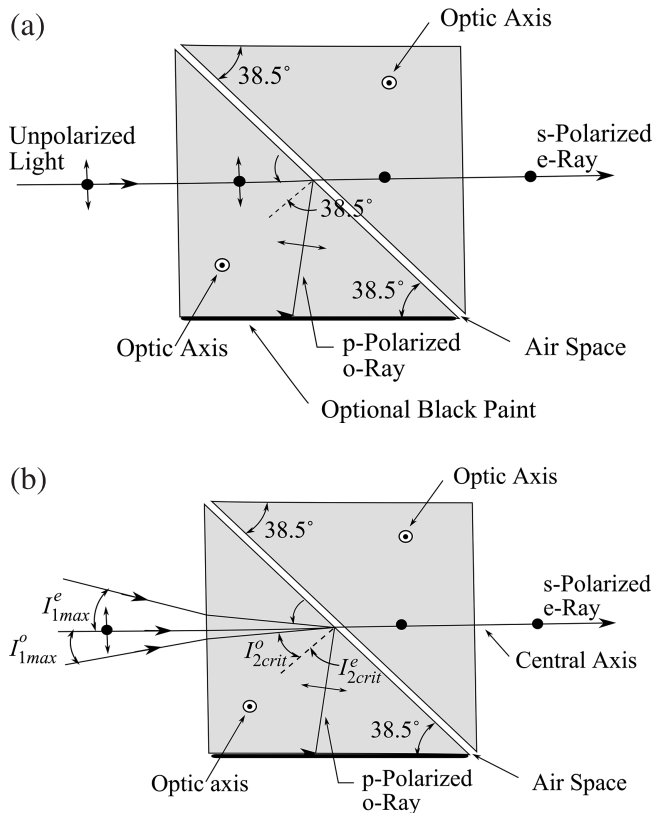


**Figure 3.3** (a) Glan–Foucault prism polarizer made of calcite,  $I_{crit}(n_o) = 37.1$  deg,  $I_{crit}(n_e) = 42.3$  deg. (b) Asymmetric field of view of Glan–Foucault prism polarizer.

Other specifications are a damage threshold of  $30 \text{ W/cm}^2$  continuous wave (CW) or  $300 \text{ W/cm}^2$  pulsed laser radiation and transmittance of s-polarized light  $> 60\%$  at  $\lambda = 633 \text{ nm}$ .

### 3.1.4 Glan–Thompson polarizing prism

The Glan–Thompson prism shown in Fig. 3.4 uses two cemented calcite prisms with each optic axis perpendicular to the plane of reflection. Using TIR separation at the glass–optical cement interface, s-polarized light is transmitted, while the reflected p-polarized light is absorbed by a blackened side face. The transmission of s-polarized light is  $> 90\%$ , and the angular field is approximately doubled to about  $12 \text{ deg}$  compared to the Glan–Foucault prism, but the Glan–Thompson prism can accept only up to  $8 \text{ W/cm}^2$  CW or  $100 \text{ W/cm}^2$  pulsed radiation due to the lower damage threshold of the optical cement.

### 3.1.5 Glan–Taylor polarizing prism

The last of the Glan group to be described here is the Glan–Taylor prism, shown in Fig. 3.5(a). Two air-spaced calcite prisms are oriented with both optic axes parallel to the plane of reflection and parallel to the entrance and exit faces. Using TIR separation, p-polarized light is transmitted, while the reflected s-polarized light is either absorbed by a blackened side face or emitted through a clear exit window. The transmission of p-polarized light is  $> 85\%$ , and the angular field is about  $6 \text{ deg}$ . It can accommodate the highest radiation level of the Glan group—up to  $30 \text{ W/cm}^2$  CW or  $500 \text{ W/cm}^2$  pulsed radiation. A modified form of the Glan–Taylor prism, shown in Fig. 3.5(b), can produce orthogonal s-polarized and p-polarized output beams. In addition, if the angle of incidence at the interface is close to Brewster's angle, there will be little reflection of p-polarized light. However, the intensity of the s-polarized reflected beam will be much less than the transmitted p-polarized beam.

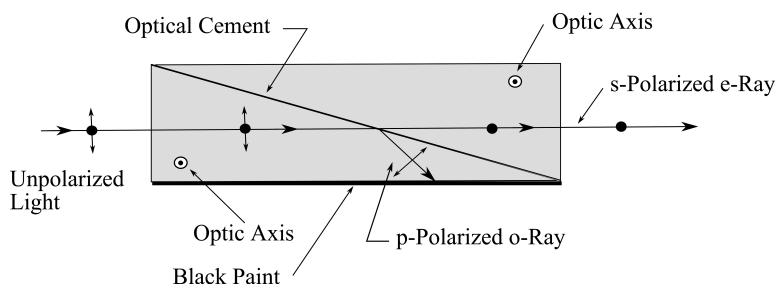


**Figure 3.4** Glan–Thompson prism polarizer made of calcite,  $I_{crit}(n_o) = 37.1 \text{ deg}$ ,  $I_{crit}(n_e) = 42.3 \text{ deg}$ .

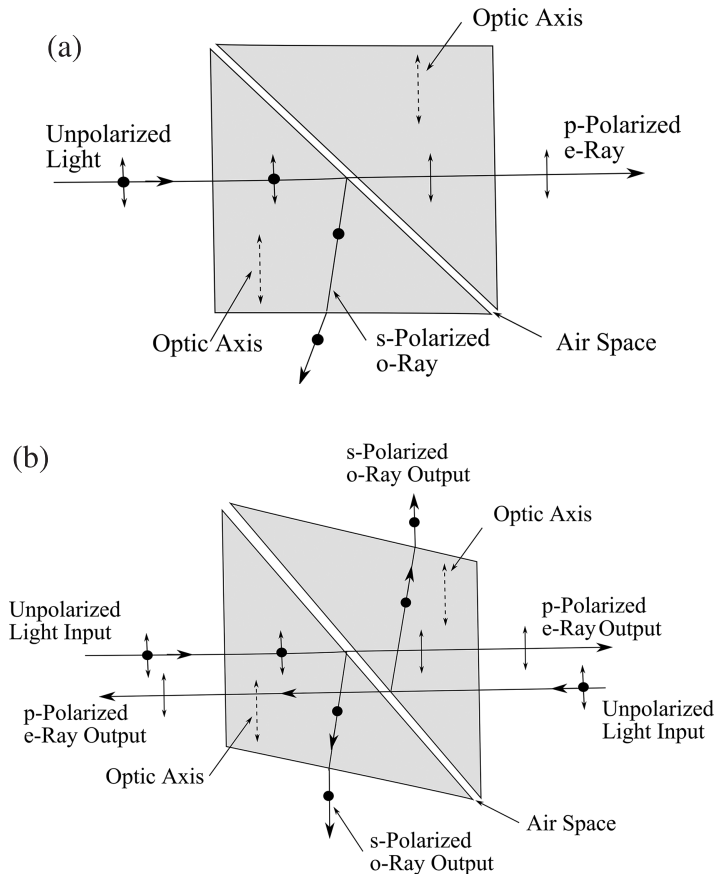


**Figure 3.5** (a) Glan–Taylor prism polarizer made of calcite. (b) Glan–Taylor prism polarizer having orthogonal outputs made of calcite.

### 3.1.6 Beam-displacing polarizing prism

Figure 3.6(a) shows a cleaved calcite rhomb where the optic axis is inclined in the principal section. Each side has corner angles  $\alpha = 78.08$  deg and  $\beta = 101.92$  deg. The optic axis direction is determined by equally trisecting a  $\beta$ - $\beta$ - $\beta$  oblique corner of the crystal. A ray enters at the edge of the principal section. The undeviated s-polarized o-ray vibrates perpendicular to the principal section, and the deviated p-polarized e-ray vibrates in the principal section, where both rays lie in the principal section. The exiting p-polarized ray is displaced and parallel to the exiting s-polarized ray. Typical exit ray separation is nominally 4 mm. This polarizing prism has the advantage that both exit beams are completely polarized and of equal intensity, although obviously the entrance beam diameter must be small. As in Fig. 3.6(b), a calcite prism pair can produce a variable beam displacement between the p-polarized and s-polarized rays.<sup>2</sup> Here, one wedge prism is slid relative to another wedge prism.

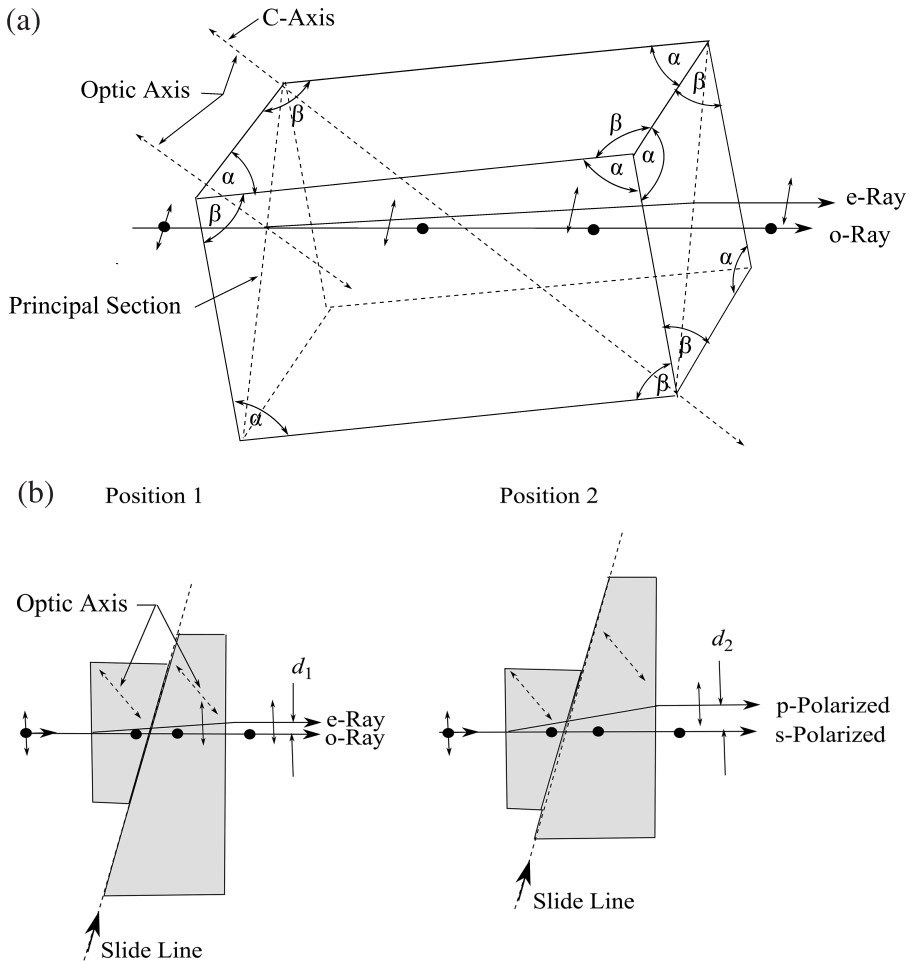


**Figure 3.6** (a) Beam-displacement prism polarizer. (b) Variable beam-displacement prism polarizer.<sup>2</sup>

### 3.1.7 Wollaston polarizing prism

Another type of beam-splitting polarizing prism is the Wollaston prism, (for William Hyde Wollaston), shown in Fig. 3.7. It usually consists of two calcite right-angle prisms optically cemented together at the hypotenuse. The optic axis of each section is orthogonal to that of the other section. An unpolarized ray traversing the first prism section is not split, but the o-ray is retarded with respect to the e-ray. The o-ray vibrates parallel to the optic axis and the e-ray perpendicular to the optic axis. Upon entering the second section, the o-ray becomes the e-ray, and vice versa. The o-ray, now slower, is bent toward the interface normal, and the e-ray is bent away from the interface normal. Prisms with a deviation angle  $\delta$  from about 5 to 45 deg between the exit beams can be obtained, depending on the right-angle prism base angles. For very high-power applications, the prisms may not be cemented together, resulting in a reduction of transmission.

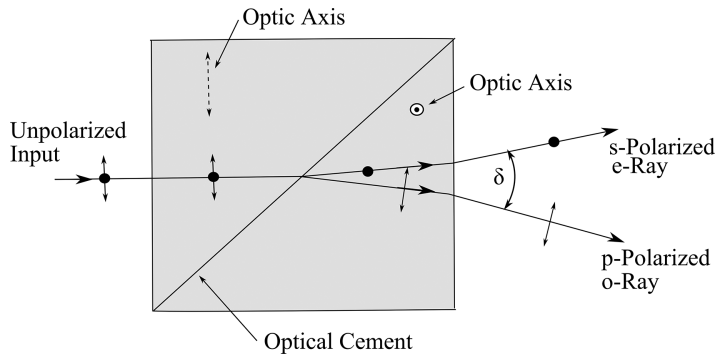


**Figure 3.7** Wollaston prism polarizer (calcite).

### 3.1.8 Nomarski polarizing prism

The Nomarski prism, named for Georges Nomarski, is a modified Wollaston prism (Fig. 3.8). The optic axis of the first right-angle calcite prism is skewed as shown, while the optic axis of the second prism is oriented the same as for the Wollaston prism. This angled optic axis causes the ordinary and extraordinary rays to intersect outside the prism, forming an interference plane. The resulting phase shifts can be detected by an analyzer. The exact distance of this interference plane from the prism is determined by the angle of the skewed optic axis and is set by the manufacturer. Normarski prisms are used in differential interference contrast (DIC) microscopes.

### 3.1.9 Rochon polarizing prism

Related to the Wollaston polarizing prism, the Rochon prism (for Alexis Marie Rochon) has the optic axis of the first calcite prism section in the direction of the incident ray (Fig. 3.9), and there is no distinction between the o-ray and the e-ray in this section. The split at the second section interface produces no deviation of the s-polarized o-ray, while the p-polarized e-ray is deviated from the interface normal. The first calcite section can be replaced by a more robust isotropic glass section, choosing a glass with a refractive index and dispersion close to either of the

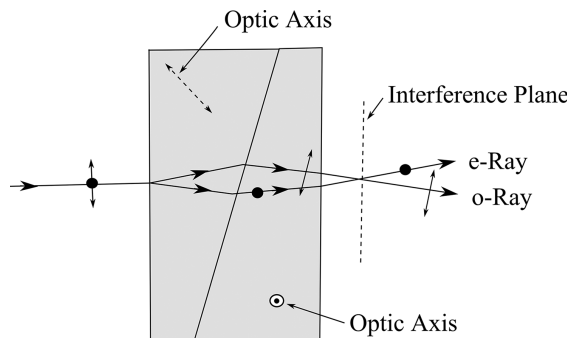


**Figure 3.8** Nomarski prism polarizer (calcite).

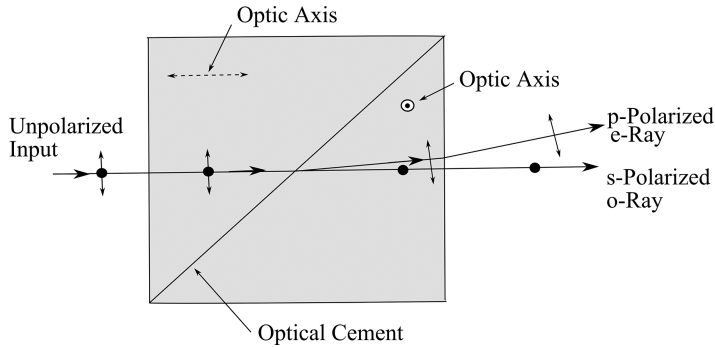


**Figure 3.9** Rochon prism polarizer (calcite).

refractive index values of calcite.<sup>3</sup> Glass-calcite Rochon prisms are commercially available using FK5 glass ( $n_d = 1.4875$ ,  $v_d = 70.41$ ), which is close to  $n_e$  and the dispersion of calcite. Typical beam-deviation angles are 5, 10, and 15 deg.

Other double-refracting crystals used in commercially available polarizing prisms are crystal quartz (circular and low birefringence), alpha-BBO ( $n_e = 1.6021$ ,  $n_o = 1.6776$  at  $\lambda = 552$  nm), YVO4 ( $n_e = 2.2154$ ,  $n_o = 1.9929$  at  $\lambda = 630$  nm), magnesium fluoride, and titanium dioxide. Polarizing prisms' surfaces are usually antireflection coated.

### 3.1.10 MacNeille polarizing beamsplitter cube

Another method to produce polarized light is by the deposition of alternating high- and low-index film layers, as described by MacNeille.<sup>4</sup> Figure 3.10 illustrates a seven-layer transparent thin-film stack having refractive indices  $n_1$  and  $n_2$ , deposited between transparent bulk material having a refractive index  $n_3$ , where  $n_1 \gg n_2$ , and  $n_1 > n_3$ . All internal rays within the layers hit the next layer at Brewster's angle. A fraction of the reflected light at each layer interface is therefore completely s-polarized. If we choose  $n_1 = 2.3$  (zinc sulfide) and  $n_2 = 1.38$

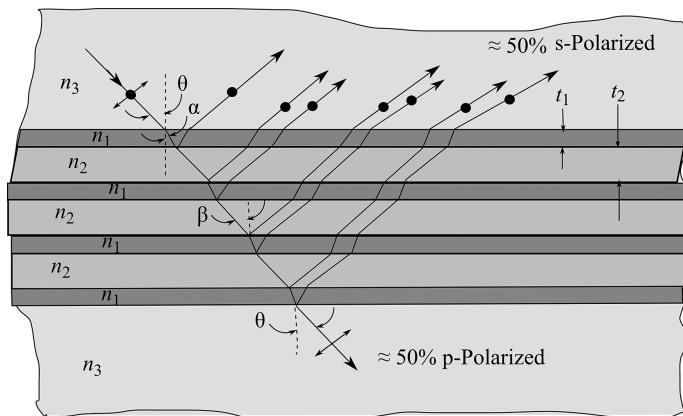


**Figure 3.10** Polarizing thin-film stack.



(magnesium fluoride), then Brewster's angles  $\alpha$  and  $\beta$  are given by

$$\alpha = \arctan\left(\frac{n_2}{n_1}\right) = 31.0 \text{ deg}, \quad (3.1)$$

$$\beta = \arctan\left(\frac{n_1}{n_2}\right) = 59.0 \text{ deg}, \quad (3.2)$$

where  $\alpha + \beta = 90$  deg and Snell's law is satisfied at each layer interface.

A useful incident angle from the bulk material to the first layer is  $\theta = 45$  deg. The required refractive index of the bulk material is then calculated from Snell's law:

$$n_3 = n_1 \left[ \frac{\sin \alpha}{\sin(45 \text{ deg})} \right] \approx 1.67. \quad (3.3)$$

Since  $\theta$  between  $n_3$  and  $n_2$  (53.9 deg) is not Brewster's angle, this incident ray is not completely s-polarized on reflection.

To maximize the intensity of the reflected s-polarized ray at each layer, the layer thickness is controlled such that the ray reflected from the next layer is in phase with the incident ray. To achieve this, the physical thicknesses  $t_1$  and  $t_2$  of the layers are controlled to be

$$t_1 = \frac{\lambda}{4 \sqrt{(n_1^2 + n_2^2)/n_1^2}}, \quad (3.4)$$

$$t_2 = \frac{\lambda}{4 \sqrt{(n_1^2 + n_2^2)/n_2^2}}, \quad (3.5)$$

where  $\lambda$  is the wavelength of the incident light, nominally 550 nm. For these seven layers, approximately 50% of the incident light is reflected as s-polarized, while the other half is transmitted as p-polarized light.

Figure 3.11 shows a 50R/50T polarizing beamsplitter (PBS) cube, where the deposited layers lie on the hypotenuse of a right-angle prism, and another right-angle prism is coupled to the hypotenuse using a thin coating of optical cement having a refractive index close to  $n_3$ . From Eq. (3.3), a suitable material for the cube would be SF5 glass ( $n_d = 1.673$ ). Both the reflected s-polarized light and the p-polarized transmitted light are at least 95% polarized over the visible spectrum, and the beamsplitter is usable for  $40 \text{ deg} \leq \theta \leq 50 \text{ deg}$ , or  $\pm 5$  deg from the ideal incident angle at the interface. The extinction ratio is the ratio of the transmitted or reflected primary polarization component to the opposite polarization component. It is possible to increase the angular field of MacNeille PBS cubes by modifying the beam-splitting coating, albeit with a reduced usable wavelength range.<sup>5</sup> Modern commercial PBS cubes of a modified MacNeille design can achieve an input  $f/\#$  down to  $\approx f/2.5$  and a transmission extinction ratio  $\approx 1,000:1$ . The minimum working  $f/\#$  of a PBS cube for projection display applications, without noticeable loss of contrast, has been stated to be  $\approx f/3.3$ .<sup>6</sup>

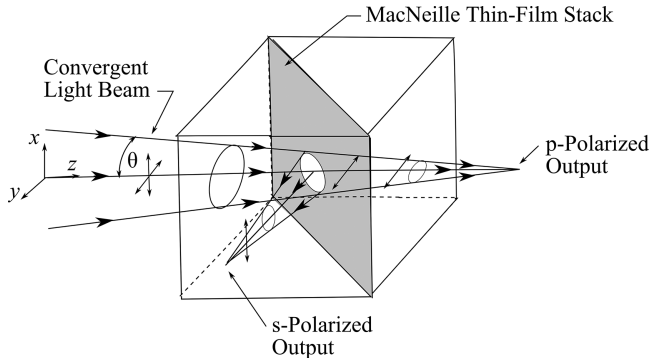


**Figure 3.11** MacNeille 50R/50T PBS cube in convergent beam of half-angle  $\theta$ .

### 3.1.11 Birefringent multilayer reflective polarizing film

A type of reflecting polarizer film has been developed by 3M that uses a multilayer stack of biaxial birefringent polymer layers.<sup>7</sup> It is designed to produce high reflectance for light with its plane of polarization parallel to one axis, and high transmission for light with its plane of polarization parallel to a second axis, both over a wide range of incident angles. A biaxial birefringent material, where the refractive indices differ along all three axes, can be produced by stretching the multilayer stack in one direction (uniaxial stretching). Figure 3.12 shows a single interface between layers for a biaxial birefringent film, and the associated refractive indices. For light incident in the  $x$ - $y$  stretch plane,  $n_{10} = n_{1x}$ ,  $n_{20} = n_{2x}$  for p-polarized light, and  $n_{10} = n_{1y}$ ,  $n_{20} = n_{2y}$  for s-polarized light. For light incident in the  $y$ - $z$  nonstretched plane,  $n_{10} = n_{1y}$ ,  $n_{20} = n_{2y}$  for p-polarized light, and  $n_{10} = n_{1x}$ ,  $n_{20} = n_{2x}$  for s-polarized light. The  $x$  direction is the extinction direction, and the  $y$  direction is the transmission direction. Typical values are  $n_{1x} = 1.88$ ,  $n_{1y} = 1.64$ ,  $n_{1z} = \text{variable}$ ,  $n_{2x} = 1.65$ ,  $n_{2y} = \text{variable}$ , and  $n_{2z} = \text{variable}$ . For the large index differential of  $1.88 - 1.65 = 0.23$  in the stretch direction, there is a high reflectance of s-polarized light for a stack of hundreds of layers, and the angular transmission of p-polarized light depends on the  $n_{1z}/n_{2z}$  index ratio.

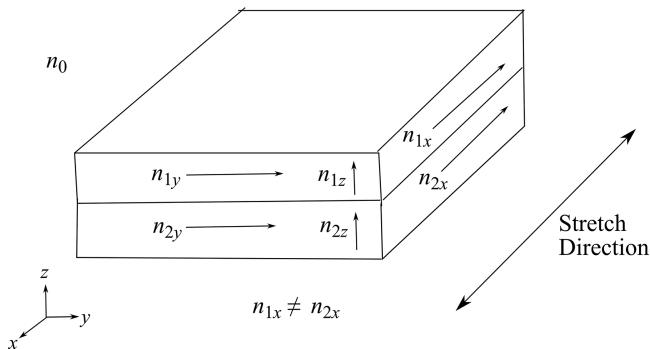


**Figure 3.12** Two-layer single interface biaxial birefringent film.